Published paper

Madsen, J, Canton, I, Warren, NJ, Themistou, E, Blanazs, A, Ustbas, B, Tian, X, Pearson, R, Battaglia, G, Lewis, AL and Armes, S.P (2013) Nile Blue-Based Nanosized pH Sensors for Simultaneous Far-Red and Near-Infrared Live Bioimaging. Journal of the American Chemical Society, 135 (39). 14863 - 14870. Doi: 10.1021/ja407380t

JACS
JOURNAL OF THE AMERICAN CHEMICAL SOCIETY
Article
pubs.acs.org/JACS

Nile Blue-Based Nanosized pH Sensors for Simultaneous Far-Red and Near-Infrared Live Bioimaging

Jeppe Madsen,*[,†,‡] Irene Canton,*[,†] Nicholas J. Warren,[‡] Efrosyni Themistou,[‡] Adam Blanazs,[‡] Burcin Ustbas,[†] Xiaohe Tian,[†] Russell Pearson,[†] Giuseppe Battaglia,[†] Andrew L. Lewis,[§] and Steven P. Armes*[,‡]

[†]Department of Biomedical Sciences, University of Sheffield, Sheffield, S10 2TN, United Kingdom
[‡]Department of Chemistry, University of Sheffield, Dainton Building, Sheffield, S3 7HF, United Kingdom
[§]Biocompatibles UK Ltd., Farnham Business Park, Weydon Lane, Farnham, GU9 8QL, United Kingdom

Supporting Information

ABSTRACT: Diblock copolymer vesicles are tagged with pH-responsive Nile Blue-based labels and used as a new type of pH-responsive colorimetric/fluorescent biosensor for far-red and near-infrared imaging of live cells. The diblock copolymer vesicles described herein are based on poly(2-(methacryloyloxy)ethyl phosphorylcholine-block-2-(diisopropylamino)ethyl methacrylate) [PMPC-PDPA]: the biomimetic PMPC block is known to facilitate rapid cell uptake for a wide range of cell lines, while the PDPA block constitutes the pH-responsive component that enables facile vesicle self-assembly in aqueous solution. These biocompatible vesicles can be utilized to detect interstitial hypoxic/acidic regions in a tumor model via a pH-dependent colorimetric shift. In addition, they are also useful for selective intracellular staining of lysosomes and early endosomes via subtle changes in fluorescence emission. Such nanoparticles combine efficient cellular uptake with a pH-responsive Nile Blue dye label to produce a highly versatile dual capability probe. This is in marked contrast to small molecule dyes, which are usually poorly uptaken by cells, frequently exhibit cytotoxicity, and are characterized by intracellular distributions invariably dictated by their hydrophilic/hydrophobic balance.

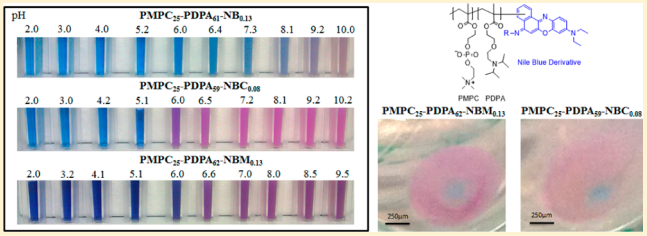

INTRODUCTION

Fluorescent probes are widely used for imaging in cell biology. Increasingly, they are also being utilized as chemosensors to diagnose specific pathological conditions and report on cellular events.[1−3] There is considerable interest in designing nanoparticles that report on physiologically relevant species such as ions,[4−6] reactive oxygen species,[7−9] gaseous biological second messengers[10−12] and hydrogen ions.[9,13,14] In particular, pH probes have diagnostic potential because many diseases are associated with changes in the local pH.[15] These include clinical and subclinical inflammation,[16] many lung-related pathologies,[17] kidney dysfunction,[18] ischemia,[19] and cancer.[20] In malignant tumors, the interstitial pH is lower than in normal tissue, and this parameter can be correlated with both poorer prognosis and weaker responses to available therapies.[21,22] This lower interstitial pH is a result of increased lactic acid production and reduced buffering and perfusion,[23] while the intracellular pH of the tumor cells typically remains at physiological levels.[24−26] Monitoring changes in the interstitial fluid within tumors is a major challenge, as most of the available probes penetrate cells and therefore only report the intracellular pH. Additional concerns associated with diagnostic probes are toxicity, targeting specificity, and signal-to-noise threshold.[27] For example, fluorescence spectroscopy and imaging are normally considered to be highly sensitive techniques, with extremely low detection limits being achieved under ideal conditions.[28] However, such sensitivity may be substantially reduced in vivo, particularly if the emission spectrum of the selected fluorophore overlaps with that of the living tissue. Thus there is considerable interest in designing new fluorescent probes based on dyes that emit in the far-red end of the visible spectrum, i.e. above 600−700 nm, in order to minimize such background interference.[29] Due to lower background interference, far red and infrared light can penetrate much more deeply into living tissue, which is beneficial for in vivo studies.[30,31]

Herein we describe a facile method for labeling polymers prepared by controlled radical polymerization techniques (e.g., atom transfer radical polymerization (ATRP) or reversible addition−fragmentation chain transfer (RAFT) polymerization) by reaction with Nile Blue-based dyes, which are found to act as polymerization spin traps.

This labeling principle was used to prepare nanoparticle-based pH sensors composed of a pH-sensitive dye label and a biocompatible pH-responsive diblock copolymer based on (2-(methacryloyloxy)ethyl phosphorylcholine) [MPC] and 2-

Received: July 27, 2013
Published: September 3, 2013

Scheme 1. Synthesis of Two Nile Blue-Based Vinyl Monomers Used in This Work[a]

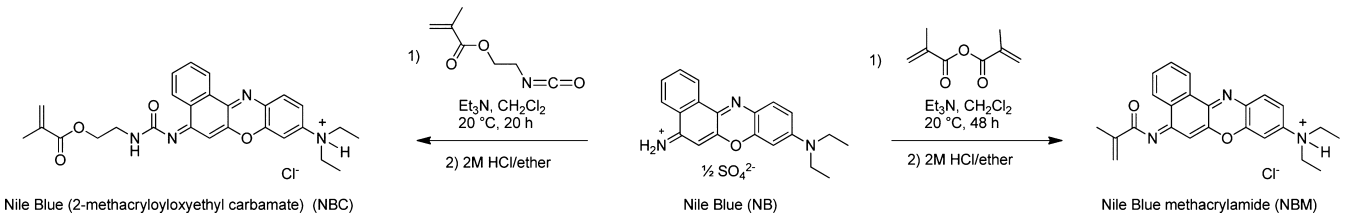

Nile Blue (2-methacryloyloxyethyl carbamate) (NBC) | Nile Blue (NB) | Nile Blue methacrylamide (NBM)

[a]Nile Blue methacrylamide (NBM) and Nile Blue 2-(methacryloyloxy)ethyl carbamate (NBC).

(diisopropylamino)ethyl methacrylate [DPA].[32,33] PMPC-based nanoparticles have been previously shown to penetrate tumors with high efficiency.[34] In addition, they can be rapidly incorporated into many different cell types and are distributed inside intracellular organelles.[35,36] The pH-sensitive probe is based on Nile Blue. Both the absorption and emission properties of Nile Blue derivatives are found to be pH-sensitive at around physiological pH.

These new nanoparticle probes report clinically relevant pH changes in tumors and cell organelles, thus enabling pH sensing both at the interstitial level (as demonstrated with multicell tumor spheroids) and also at the subcellular level.

RESULTS AND DISCUSSION

Synthesis of Nile Blue Dye Derivatives. The synthesis of the Nile Blue methacrylamide (NBM) and Nile Blue 2-(methacryloyloxy)ethyl carbamate (NBC) monomers used in this work is summarized in Scheme 1. Both monomers have been previously prepared by similar synthetic routes.[37,38] These methacrylic dyes were used as prepared for copolymerizations, but were further purified using column chromatography in order to assess their spectroscopic properties (Table S1 of the Supporting Information, SI). Dye purity before and after column chromatography was assessed using HPLC (Table S1 of the SI). Each monomer was characterized by absorption spectroscopy studies in ethanol (Table S1 and Figure S1 of the SI). Both the absorption coefficient at λ_{max} and the integral absorption coefficient[39] were determined for each dye label and found to be close to the values measured for a commercially available Nile Blue dye precursor (95% purity, laser grade), which suggests high purities for these Nile Blue-based monomers (Table S1 of the SI).

Scheme 2. Deprotonation of (a) NB, (b) NBM, and (c) NBC[a]

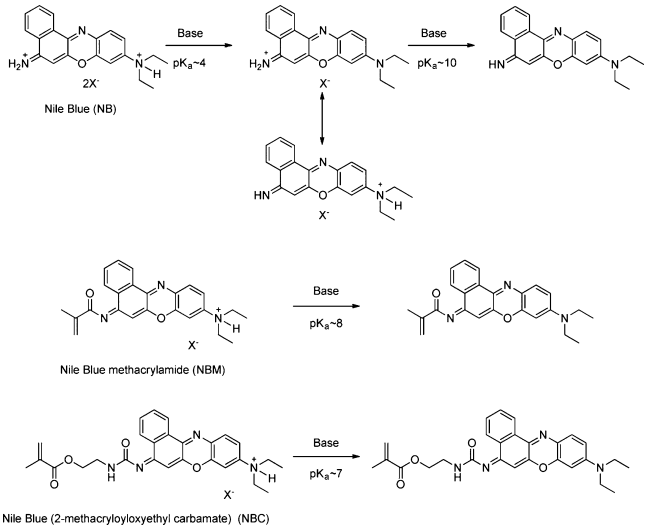

[a]The monocationic form of Nile Blue is stabilized by resonance, thereby increasing its pK_a to around 10. In contrast, NBM and NBC cannot form such resonance structures, thus their pK_a values are correspondingly lower.

Dye-Labeling of PMPC. In initial experiments, it was found that statistical copolymerization of MPC with small quantities of either NBC, NBM, or NB via Atom Transfer Radical Polymerization (ATRP) afforded dye-labeled copolymers with somewhat lower dye contents than those targeted (Table S2 of the SI). This protocol also significantly retarded the overall rate of copolymerization (Figure S2 of the SI). Similar retardation/inhibition was also observed when attempting to copolymerize NBM and NBC using reversible addition–fragmentation chain transfer (RAFT) polymerization (Figure S3 of the SI). With the benefit of hindsight, Nile Blue is structurally similar to well-known polymerization inhibitors such as methylene blue or phenothiazine (Figure S4 of the SI). Thus it seems that these Nile Blue derivatives act as spin traps during their copolymerization with MPC, leading to retardation effects (Figure S5 of the SI).[40] We hypothesized that well-defined Nile Blue-labeled polymers could be conveniently prepared by reacting Nile Blue with the propagating polymer radicals, thus quenching the polymerization and leading to a terminally attached dye label (see Figure S5 A, eq 7 of the SI). This hypothesis is supported by literature data for the reaction of phenothiazine and related compounds with alkyl radicals.[41] This suggests that the rate of reaction between alkyl radicals and vinyl monomers is at least as fast (or faster) as that between alkyl radicals and phenothiazine-like compounds. On the basis of the results described in ref 41 and also data obtained for the polymerization of aniline[42] the quenched polymer chain is most likely conjugated to the Nile Blue via its iminium nitrogen (see Figure S5B of the SI), but further mechanistic details are beyond the scope of the present study. For NBM, reaction with the double bond seems likely, which would produce a persistent radical that is stabilized via conjugation. For NBC, reaction with the double bond could lead to an intramolecular reaction with the aromatic ring, leading to a stabilized radical. Thus Nile Blue *precursor* was added to a MPC *homopolymerization* at a monomer conversion of around 70–80% (Table S2, entry 7 of the SI). This protocol minimizes the problem of retardation and hence improves the overall yield: the dye label reacted with 8% of the PMPC chains, which were of relatively low polydispersity. The NBM and NBC comonomers were also added to separate MPC homopolymerizations at similarly high conversions (see Table S2, entries 5 and 6, respectively, of the SI). In these latter syntheses, the dye label can be incorporated via copolymeriza-

dx.doi.org/10.1021/ja407380t | J. Am. Chem. Soc. 2013, 135, 14863–14870

Scheme 3. Atom Transfer Radical Polymerization (ATRP) Synthesis of PMPC-PDPA Diblock Copolymers Terminated with Either Nile Blue (NB) Alone or Containing a Nile Blue-Based Comonomer (Either NBM or NBC)[a]

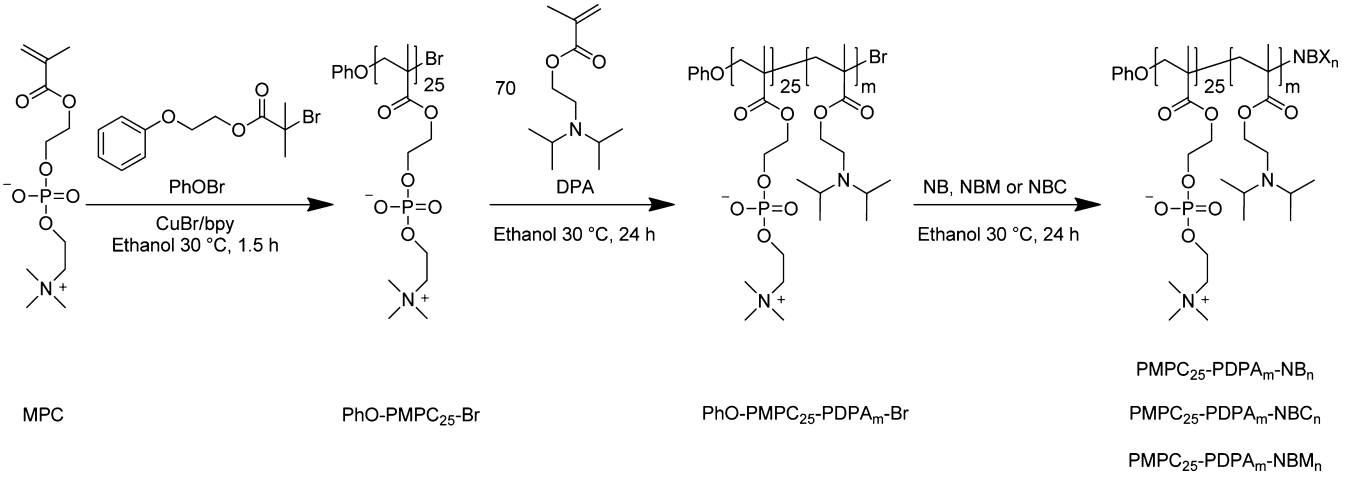

[a]In each synthesis, the Nile Blue-based reagent was added after approximately 80% conversion of the DPA monomer, as judged by ^{1}H NMR spectroscopy.

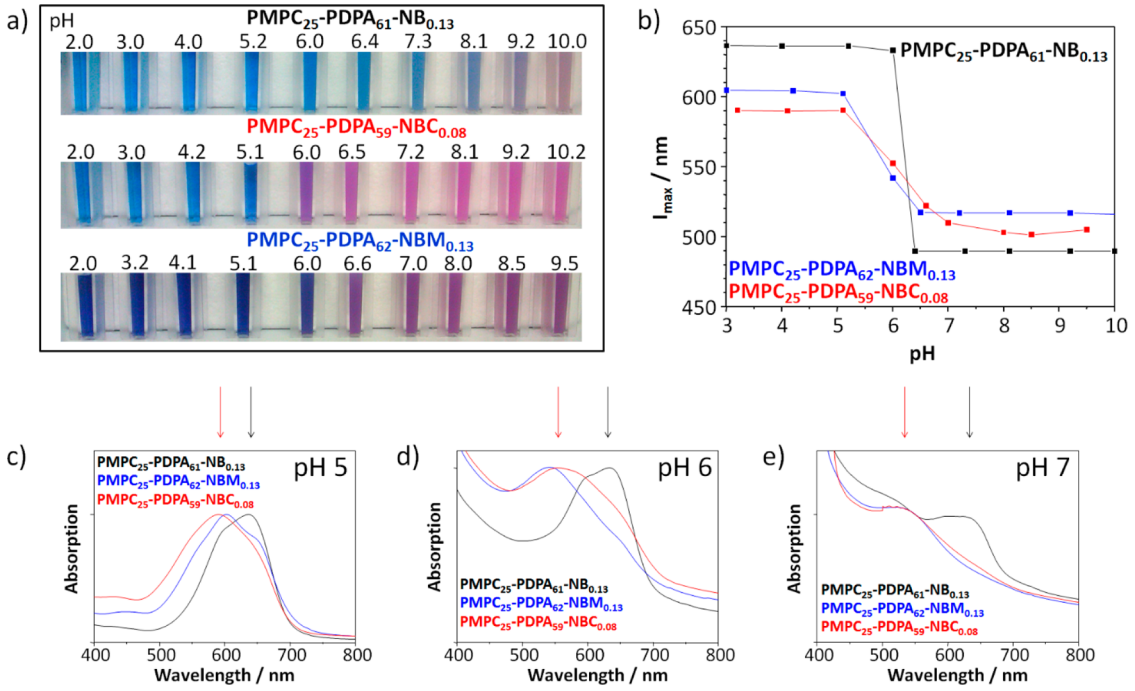

Figure 1. Visible absorption characteristics of three $PMPC_{25}PDPA_{59}NBC_{0.08}$, $PMPC_{25}PDPA_{62}NBM_{0.13}$ and $PMPC_{25}PDPA_{61}NB_{0.13}$ diblock copolymers as a function of pH. (a) Digital photographs obtained for 5 mg/mL aqueous copolymer solutions in 1 cm cuvette cells. (b) Variation of λ_{max} with solution pH. (c) Absorption spectra recorded at pH 5. (d) Absorption spectra recorded at pH 6. (e) Absorption spectra recorded at pH 7. Spectrometer settings: Scan speed = 200 nm min^{-1}; bandwidth = 1.5 nm.

tion, as well as acting as a chain transfer agent. Thus the final dye contents were slightly higher when using NBM and NBC, compared to that achieved for Nile Blue alone (compare entries 5, 6, and 7 in Table S2 of the SI). However, the conjugated dye content never exceeded 16 mol % of the added dye, so extensive dialysis was required to remove non-conjugated dye (see SI).

Furthermore, the rate of ATRP or RAFT copolymerization decreases in the presence of each Nile Blue monomer (Figures S2 and S3 of the SI) and no significant increase in monomer conversion was found by ^{1}H NMR spectroscopy when the dye was added at high conversion (data not shown). These observations suggest that all three vinyl-functional dyes actually act mainly as chain transfer agents, rather than as comonomers.

Absorption and Emission Properties of Dye-Labeled PMPC Homopolymers. The maximum *emission* wavelength of all labeled PMPC homopolymers in PBS at pH 7.2 was within 20 nm of 674 nm, the literature value reported for Nile Blue (Table S2 of the SI).[43] However, the maximum *absorption* wavelength shifted to around 590 nm for homopolymers labeled with NBM and NBC. In contrast, homopolymers terminated using unmodified Nile Blue *precursor* had a maximum absorption wavelength close to 650 nm in PBS. (Table S2 and Figure S7 of the SI). Relative quantum yields

dx.doi.org/10.1021/ja407380t | J. Am. Chem. Soc. 2013, 135, 14863−14870

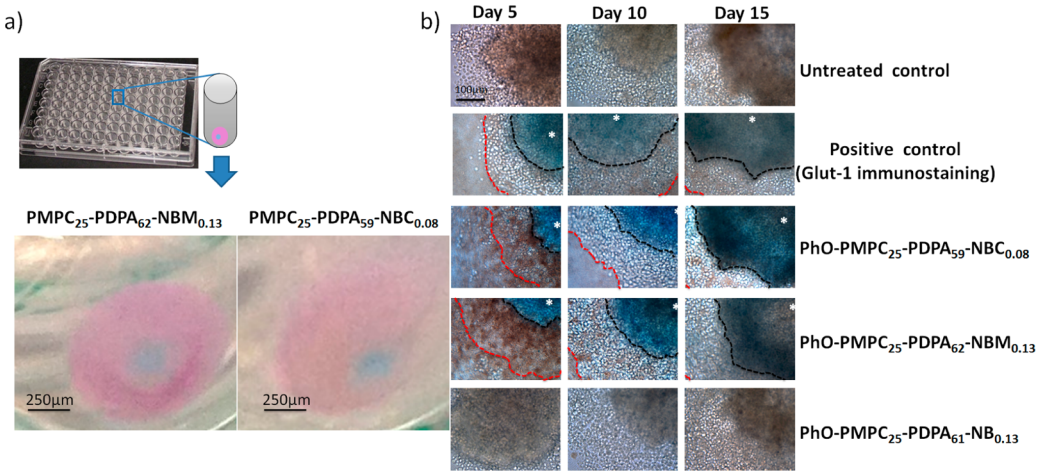

Figure 2. (a) Ultralow attachment 96-well plate model for the growth of multicellular tumor spheroids (MCTS), which were exposed to 1.0 g/L Nile Blue labeled PMPC-PDPA diblock copolymers for 36 h and corresponding digital photographs recorded for two wells containing 15-day-old MCTS after exposure to the copolymer nanoparticles for 36 h. (b) pH-Dependent staining of MCTS by Nile Blue-labeled PMPC-PDPA copolymers. Bright-field optical images of Nile Blue-labeled copolymer-treated MCTS and controls were recorded using a Leica DMI4000B instrument equipped with a Nuance Multispectral imaging System. Untreated control spheroids were used to subtract the background noise from these images. Image analysis was performed double-blinded. Four independent observers were asked to score the center of the tumor (white star), the edge (red dotted line) and whether the observer could identify the boundary for the color change (black dotted line). Hypoxic (low pH) regions of the spheroids were compared to a positive control marker for hypoxia (Glut-1 immunostaining).

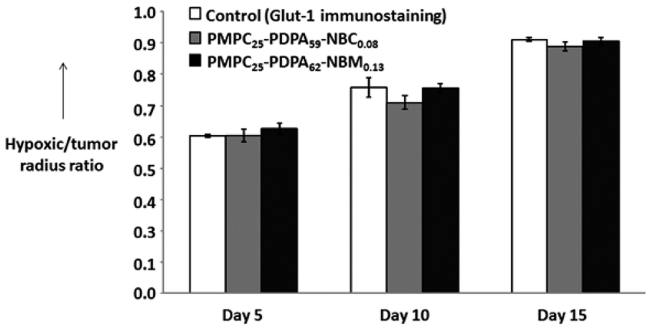

Figure 3. Monitoring the reduction in local pH within multicellular tumor spheroids (MCTS) over time using Nile Blue-labeled PMPC-PDPA diblock copolymer vesicles. MDA-MB-231 breast tumor spheroids were grown on ultralow adhesion 96-well plates. These MCTS samples were treated with 1.0 g/L of PMPC-PDPA vesicles for 36 h and then imaged using an optical microscope (Leica Caliper LS, 20X, which corresponds to approximately 25% of the total area of an MCTS). Micrographs were analyzed de viso (see Figure 2b) and the radii of the hypoxic (blue, acidic) areas of the spheroids were compared to the overall MCTS radii. The hypoxic/tumor radius ratio was monitored over time for 5, 10, or 15 days. Immunolabeling of Glut-1 was used as a control for fixed spheroid hypoxia. Data are expressed as mean radius ratios for $N = 3$ independent experiments ± SEM.

were determined for all Nile Blue-labeled homopolymers in PBS at pH 7.2 (Table S2 of the SI). NBM-labeled chains had relatively low quantum yields, comparable to that of Nile Blue. However, Nile Blue-terminated PMPC chains generally gave higher quantum yields. This agrees with previous literature reports suggesting that solubilizing groups (in this case the PMPC chain) suppress dye aggregation in aqueous solution.[43,44] If NBC was used as a comonomer, then relative quantum yields are generally one order of magnitude greater than for Nile Blue (Table S2 of the SI). Similarly high quantum yields have been reported for deprotonated Nile Blue (Scheme 2).[45]

The pH-dependent fluorescence of dye-labeled PMPC homopolymers was examined (see Figures S8 and S9 of the SI). Chains labeled with unmodified Nile Blue exhibited a low emission intensity below pH 3, and enhanced emission above pH 8. Stronger emission in alkaline solution suggests deprotonation of the Nile Blue (see Scheme 2a).[46] Reduced emission observed in acidic solution is most likely related to protonation of Nile Blue at the second nitrogen on the ring.[47] As shown in Scheme 2a, monocationic Nile Blue is resonance-stabilized, which accounts for its unusually high pK_a compared to other aromatic amines such as aniline.[48] The fluorescence behavior of the PMPC homopolymers labeled with either NBM or NBC exhibits pH-sensitivity in the physiological region (Figures S8 and S9 of the SI). Below pH 6, a single emission band was observed at 670 nm for $PMPC_{41}NBM_{0.16}$. Above pH 6, a new band appeared at around 700 nm. The 700/670 nm emission intensity ratio increased significantly at higher pH for $PMPC_{41}$-$NBM_{0.18}$, whereas this ratio remained essentially constant for PMPC chains labeled with either NB or NBC (Figure S9 of the SI). In contrast, the integrated emission intensity of $PMPC_{41}NBC_{0.10}$ increased by one order of magnitude between pH 5 and pH 8 (Figure S9 of the SI). This strongly enhanced emission is consistent with the higher quantum yields found for this particular polymer (Table S2 of the SI). Studies of lipophilic Nile Blue derivatives with chemical structures similar to NBM and NBC have reported lower pK_a values than for nonmodified Nile Blue.[49] This is probably due to the electron-withdrawing effect of the carbonyl substituent on the imine nitrogen, which destabilizes the monocationic derivatives relative to unmodified Nile Blue. Such destabilization leads to lower pK_a values that are comparable to those found for other aromatic amines such as aniline[48] (see Scheme 2).

The spectral changes observed for PMPC chains labeled with NBM and NBC occur at slightly lower pH values compared to those found for the NBM and NBC monomers (Figures S9 and S10 of the SI). Moreover, the fluorescence intensity of the labeled homopolymers increases at higher pH. This is in

dx.doi.org/10.1021/ja407380t | J. Am. Chem. Soc. 2013, 135, 14863−14870

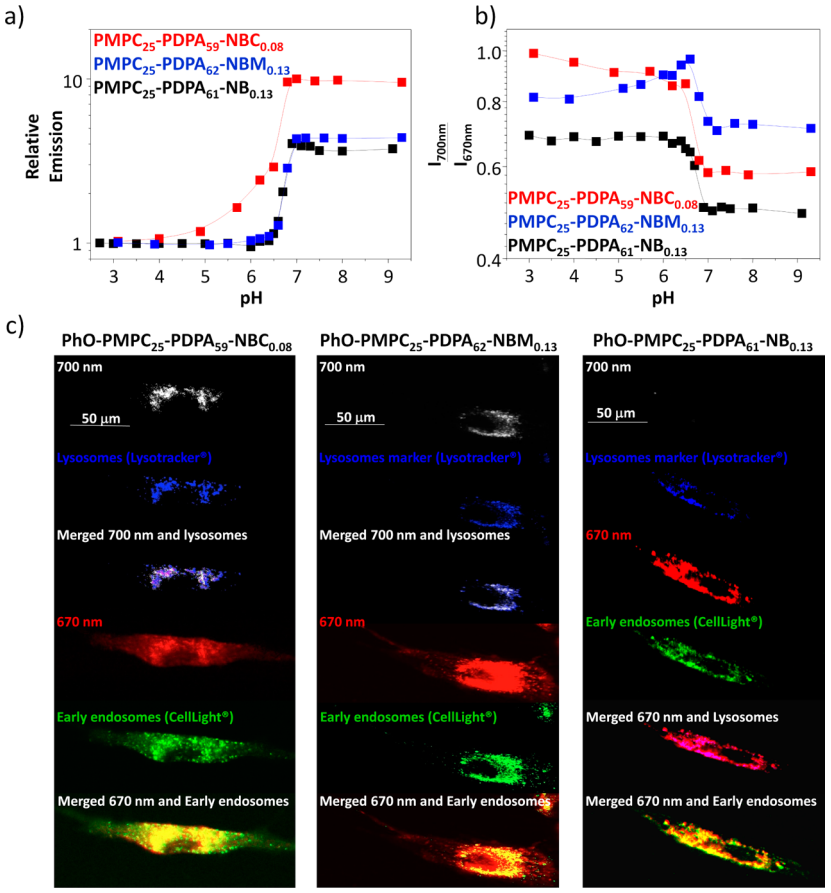

Figure 4. (a) Fluorescence intensity vs pH for 1.0 g/L aqueous solutions of Nile Blue-labeled PMPC-PDPA diblock copolymers recorded at an excitation wavelength of 550 nm. (b) Fluorescence emission intensity ratio (700/670 nm; excitation wavelength = 550 nm) vs pH for 1.0 g/L aqueous solutions of Nile Blue-labeled PMPC-PDPA copolymers. (c) Subcellular fluorescent staining of organelles in live cells by Nile blue-labeled PMPC-PDPA copolymers. Primary human dermal fibroblasts were treated with a 1.0 g/L aqueous solution of each of the three copolymers for 24 h. Fluorescence micrographs were recorded to identify the subcellular signal of the copolymers (λ_{ex} (550 nm)/λ_{em} (670 nm); λ_{em} = 700 nm). Each copolymer signal was colocalized with the following conventional subcellular markers: early endosome marker for Rab-5 (CellLight Early Endosomes-GFP, Invitrogen) and lysosomal marker (Lysotracker, Invitrogen). The amphiphilic PMPC-PDPA diblock copolymer diffuses throughout the subcellular region, but accumulates preferentially at membrane surfaces. The local pH of the lysosomes is below pH 5, whereas the local pH of the early endosomes is around pH 6–7. Thus the two Nile Blue comonomer labels report both the presence and the chemical state of the copolymer, with the latter being sensitive to the local pH due to the pH-responsive nature of the PDPA block. In contrast, if the Nile Blue label is incorporated as a chain transfer agent, rather than as a comonomer, then the copolymer fluorescence is insensitive to the local pH.

striking contrast to the behavior of the corresponding monomers, for which a *reduction* in intensity is observed at higher pH. However, the deprotonated forms of NBM and NBC are stabilized in aqueous solution when conjugated to a highly hydrophilic PMPC chain, which explains the lower pH transition. In contrast, the corresponding deprotonated monomers have relatively low aqueous solubilities, similar to what has previously been observed for structurally related lipophilic Nile Blue derivatives.[49] Therefore, the polymerized fluorophores are significantly more fluorescent in aqueous solution than their vinyl monomer counterparts (Figure S9 of the SI)

Dye-Labeled PMPC-PDPA Diblock Copolymers. Although the pH-sensitive emission of the labeled homopolymers occurs within a pH range that is physiologically relevant, PMPC homopolymers do *not* enter cells (Figure S11 of the SI).[50] Therefore, in order to exploit this unexpected pH-dependence, three pH-responsive PMPC-PDPA diblock copolymers[32] were prepared using either NB, NBC, or NBM (Scheme 3). In each case, the PMPC block was used as a macroinitiator and the dye label was added at relatively high DPA conversion (around 80%). Vesicle-forming pH-responsive PMPC-PDPA diblock copolymers with similar compositions have been previously used for both in vitro and in vivo drug delivery.[33−35,51,52] The effect of varying the solution pH on the absorption of the three labeled pH-responsive diblock copolymers is shown in Figure 1. Raising the pH did not lead to a significant change in the color of the $PMPC_{25}$-$PDPA_{61}$-$NB_{0.13}$ solution/dispersion up to pH 9, whereas a distinct color change from blue to purple was observed between pH 5 and 6 for $PMPC_{25}PDPA_{59}NBC_{0.08}$ and between pH 6 and 7 for $PMPC_{25}PDPA_{62}NBM_{0.13}$ (Figure 1a). Deprotonation of the PDPA block, which occurs just above pH 6, leads to in situ self-assembly to form diblock copolymer vesicles.[32] The vesicle membranes comprise PDPA chains, which provide a highly hydrophobic environment that shifts the absorption wavelength of the Nile Blue label and increases its quantum yield.[41,43] Figure 1b shows how λ_{max} varies with pH for all three copolymers. The λ_{max} observed for $PMPC_{25}PDPA_{61}NB_{0.13}$ decreases sharply from 640 to 585 nm between pH 6.0 and pH 6.4. This pH range corresponds approximately to the known pK_a of the PDPA block.[32] Close examination of the

dx.doi.org/10.1021/ja407380t | J. Am. Chem. Soc. 2013, 135, 14863−14870

absorption spectra at pH 5, 6, and 7 (Figure 1c-1e) reveals an additional feature at around 485 nm, which corresponds to the peak assigned to deprotonated Nile Blue within reverse micelles reported by Das et al.[41] However, in the spectrum recorded at pH 7 a 640 nm peak is still visible, despite the strong light scattering caused by vesicle formation (Figure 1e). This latter feature corresponds to protonated Nile Blue, and was also observed for the reverse micelle system described by Das et al.[41] The residual protonated Nile Blue is responsible for the absence of any color change in the copolymer solutions (Figure 1a). In contrast, the λ_{max} is reduced much more gradually from around 600 nm at pH 5 to around 500 nm at pH 7 for both $PMPC_{25}PDPA_{59}NBC_{0.08}$ and $PMPC_{25}PDPA_{62}NBM_{0.13}$ (see Figure 1b). Inspection of the absorption spectra obtained for these two copolymers show one dominant peak that shifts between pH 5 and 7 (see Figure 1c-1e). In this case, there is no residual peak from the protonated dye and the color shift is much more pronounced for these two copolymer solutions (see Figure 1a).

Toxicity of Dye-Labeled PMPC-PDPA Block Copolymers. Vesicle biocompatibility studies of the three Nile Blue-labeled PMPC-PDPA diblock copolymers were performed on human dermal fibroblasts (Figure S13 of the SI). High cell viabilities were obtained, which is consistent with those previously observed for PMPC-PDPA diblock copolymers.[33,36]

Use of Dye-Labeled PMPC-PDPA Block Copolymers for Monitoring Hypoxic Regions in Tumor Models. The sensitivity of the three Nile Blue-labeled PMPC-PDPA diblock copolymers to the local pH within a multicell tumor spheroid (MCTS) model was evaluated. Given its marked gradients in pH,[53] oxygen, and glucose concentration between the outer and inner regions,[54,55] the MCTS model is generally considered to be a superior mimic for the physiological changes that occur in avascular tumor tissues compared to cell monolayers.[56] Figure 2 confirms that the pH-sensitivity of $PMPC_{25}PDPA_{59}NBC_{0.08}$ and $PMPC_{25}PDPA_{62}NBM_{0.13}$ enables the local pH to be conveniently monitored within MCTS tissue. Culturing of MCTS for 5, 10, or 15 days allowed tissue growth, thus increasing the area of the hypoxic region over time. For comparative assessment of the probes, immunostaining of glucose transporter 1 (Glut-1) in MCTS was performed as a positive control (see Figure 2b). This approach is well established for fixed (dead) tissue, but is not applicable for live tissue. Glut-1 expression has been reported to correlate well with tumor hypoxia both in vivo[57] and in MCTS models.[58] In the latter case, its use results in a gradient of increasing intensity toward the center of the spheroid. For copolymer-treated MCTS, the growth of the hypoxic region could be directly visualized by a change in the color of the stained spheroid tumor tissue from purple (physiological pH) to blue (low pH), as indicated by the digital photographs shown in Figure 1a. In addition, the boundary between low pH and physiological pH within the spheroid mass could be accurately determined using optical microscopy (see Figure 2b).

Both $PMPC_{25}PDPA_{62}NBM_{0.13}$ and $PMPC_{25}PDPA_{59}NBC_{0.08}$ probes were able to detect pH changes within the living tissue (i.e., between the inner and outer edges) over time in a similar manner to the positive control performed using Glut-1 on fixed tissue (see Figure 3). It is worth emphasizing that, although PMPC-PDPA diblock copolymer vesicles are rapidly uptaken by most cell types,[33,36] a significant fraction will nevertheless remain within the interstitial tissue. When the PDPA block becomes highly protonated below approximately pH 6.0, vesicle dissociation occurs. The resulting individual copolymer chains are uptaken to a lesser extent than the vesicles, and a relatively large fraction of the former species does not enter cells in hypoxic (acidic) tissue. Although the copolymer chains acquire cationic character and in principle may bind electrostatically to negatively charged cell membranes, internalization does not occur unless the local concentration of cationic charge density becomes high enough to disrupt the membrane.[59,60] The relatively small size of the copolymer chains[61] also makes endocytosis unlikely, and this process is further hindered by the acidic environment.[62] Therefore, these new biocompatible Nile Blue-based copolymer probes enable the differential interstitial pH of live spheroids to be monitored continuously and noninvasively in real time, as opposed to the indirect approach required for fixed tissue based on Glut-1. This is important because, although the interstitial pH decreases, the intracellular pH remains at physiological levels in tumoral masses.[25,26,63] Importantly, no differential staining was observed when the MCTS model was treated with $PMPC_{25}-PDPA_{61}-NB_{0.13}$ (Figure 2). This is consistent with our observation of a minimal spectral shift for this copolymer over the pH range of interest (Figure 1a,c).

Dye-Labeled PMPC-PDPA Copolymers As Fluorescent Probes of Intracellular Environments. Figure 4a shows the fluorescence intensity as a function of solution pH. For all copolymers, the emission intensity increases at higher pH, but the onset of this stronger fluorescence occurs between pH 4 and 5 for $PMPC_{25}PDPA_{59}NBC_{0.08}$, whereas it is observed at around pH 6.5 (i.e., close to the PDPA pK_a) for the other two copolymers. Deprotonation of the PDPA block provides a hydrophobic environment, which is known to increase the quantum yield of Nile Blue.[43,45] The 700 nm/670 nm emission *ratio* is also pH-dependent (see Figure 4b). This parameter decreases for $PMPC_{25}PDPA_{61}NB_{0.13}$ at around the pK_a of the PDPA block. A hypsochromic shift from 660 to 575 nm in the emission spectra (Figure S12 of the SI) is consistent with formation of the deprotonated form of Nile Blue in the hydrophobic vesicle membranes formed by the neutral PDPA blocks.[45] This dominates the emission spectra due to the increased quantum yield, although the absorption spectra shows that there is still a significant amount of protonated dye (see Figure 1).

Similar behavior is observed for $PMPC_{25}PDPA_{59}NBC_{0.08}$ but the shift is only 40 nm in this case (see Figure S12 of the SI). $PMPC_{25}PDPA_{62}NBM_{0.13}$ has a maximum emission ratio at pH 6.5; this is attributed to the additional band in the emission spectrum of NBM (Figure S8 of the SI), which enhances the fluorescence intensity at 700 nm.

However, in situ formation of the vesicle membranes provides a hydrophobic environment that shifts the maximum emission wavelength, which offsets this effect. This leads to an overall reduction in emission ratio above pH 6.5 (see Figure 4b). Nevertheless, the observed shift in emission due to the more hydrophobic local environment is significantly less for NBM and NBC than for NB. PMPC-PDPA vesicles are readily uptaken by cells and become uniformly distributed within membrane organelles.[33,36] As shown in Figure 4c, exposure of cells to both $PMPC_{25}PDPA_{59}NBC_{0.08}$ and $PMPC_{25}PDPA_{62}-NBM_{0.13}$ led to colocalization of the 700 nm signal with lysosomes (pH < 5). In addition, early endosomes could be detected using the 670 nm signal (pH 6.0−6.5). The higher relative ratio observed at around pH 6.5 of $PMPC_{25}PDPA_{62}-NBM_{0.13}$ allows other intracellular regions to be visualized, as

dx.doi.org/10.1021/ja407380t | J. Am. Chem. Soc. 2013, 135, 14863−14870

shown in the merged image. $PMPC_{25}PDPA_{61}NB_{0.13}$ could not be detected at 700 nm (Figure 4c), due to the relatively weak fluorescence of this polymer at this wavelength. Instead, the 670 nm signal was uniformly distributed within the cell, regardless of the pH of the subcellular localization. This indicates the uniform localization of this copolymer, as previously observed with rhodamine-labeled copolymers.[36]

CONCLUSIONS

In summary, Nile Blue-based vinyl monomers act as spin-traps, retarding living radical polymerizations. Nevertheless, labeled polymers can be prepared by adding the dye label at high polymer conversion, albeit with relatively low labeling efficiency. Such Nile Blue labels can be incorporated into PMPC-PDPA diblock copolymers, which then self-assemble to form biocompatible vesicles at physiological pH. These copolymers exhibit variable absorption and fluorescence emission depending on their local pH. Importantly, they can be utilized for imaging pH gradients within live tumor models, as well as for probing intracellular microenvironments. This principle is summarized in Figure 5. The advantage of this new probe is that the nature of the copolymer determines its biological fate, while the fluorophore reports on the local pH. In contrast, the cellular uptake and intracellular localization of small molecule probes is mainly dictated by their hydrophilic/hydrophobic balance. Thus, uptake of hydrophobic molecules by cells is usually rather slow and inefficient.[64−68] In view of the wide range of pathological conditions that are characterized by a pH imbalance, such copolymers are expected to have a broad range of applications. Finally, such copolymer vesicles can also encapsulate both hydrophilic and hydrophobic drugs[36,69] which suggests their potential use as theranostic agents.

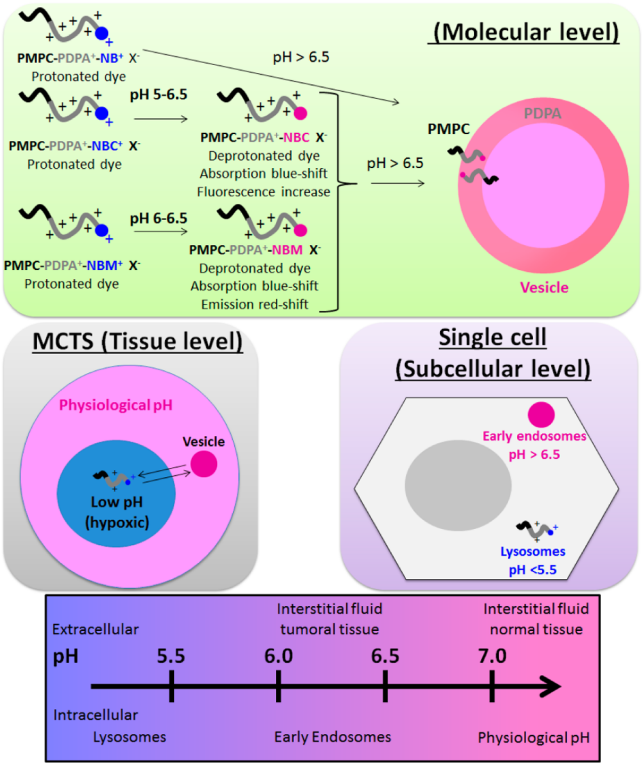

Figure 5. Schematic representation of the basic principle for using Nile Blue-labeled PMPC-PDPA copolymer vesicles as pH-sensitive probes. At low pH, both the PDPA block and the dye label are protonated, and the copolymer chains are molecularly dissolved. Above pH 5−6, deprotonation of the copolymerized Nile Blue labels (NBC or NBM) occurs. Thus the $PMPC_{25}PDPA_{59}NBC_{0.08}$ and $PMPC_{25}PDPA_{62}$-$NBM_{0.13}$ diblock copolymers exhibit a shift in both absorption and emission (see Figure 1 and Figure 4). PMPC-PDPA labeled with unmodified Nile Blue behaves differently because of the much higher pK_a of this fluorophore. Above pH 6.5, vesicles are formed in all cases because the deprotonated PDPA block becomes hydrophobic. Exposure of these vesicles to MCTS tumor spheroids leads to their dissociation and *colorimetric staining* of the *interstitial* tissue due to the lower pH, because molecularly dissolved copolymer chains are not readily uptaken by cells. However, if the tissue is non-hypoxic the PMPC-PDPA vesicles remain intact at around physiological pH. It is well-known that such vesicles are rapidly uptaken by many cell lines.[35] The pH-dependent *fluorescence* of the NBM- and NBC-labeled copolymers (Figure 4) can be used to monitor intracellular compartments because such PMPC-PDPA copolymers are known to be uniformly distributed over all intracellular membranes.[36] Hence the nature of the copolymer determines the spatial location of the pH probe.

ASSOCIATED CONTENT

Supporting Information

Detailed synthetic protocols, measured data of all prepared compounds, absorption and emission spectra vs pH, kinetic data, and toxicity data. This material is available free of charge via the Internet at http://pubs.acs.org.

AUTHOR INFORMATION

Corresponding Author

s.p.armes@shef.ac.uk

Author Contributions

I.C. and J.M. contributed equally to this work.

Notes

The authors declare no competing financial interest.

ACKNOWLEDGMENTS

EPSRC is acknowledged for funding of Postdoctoral fellowships for J.M. (Grant No. EP/G062137/1) and I.C. (Grant No. EP/I001697/1). S.P.A. acknowledges an ERC Advanced Investigator grant (PISA 320372). YCR (SPP062) is acknowledged for the development of the MCTS model and for funding B.U. We would like to thank Mr. Adrian Joseph for his help with imaging and Prof. Matthew Holley for helpful discussions. The three reviewers of this manuscript are acknowledged for their helpful comments.

REFERENCES

(1) Nadler, A.; Schultz, C. *Angew. Chem., Int. Ed.* **2013**, *52*, 2408−2410.

(2) Schäferling, M. *Angew. Chem., Int. Ed.* **2012**, *51*, 3532−3554.

(3) Lee, N. S.; Sun, G.; Neumann, W. L.; Freskos, J. N.; Shieh, J. J.; Dorshow, R. B.; Wooley, K. L. *Adv. Mater.* **2009**, *21*, 1344−1348.

(4) Lin, X.; Xie, J.; Zhu, L.; Lee, S.; Niu, G.; Ma, Y.; Kim, K.; Chen, X. *Angew. Chem., Int. Ed.* **2011**, *50*, 1569−1572.

(5) Choi, Y.; Park, Y.; Kang, T.; Lee, L. P. *Nat. Nanotechnol.* **2009**, *4*, 742−746.

(6) Li, C.; Liu, S. *Chem. Commun.* **2012**, *48*, 3262−3278.

(7) Zolnik, B.; Potter, T. M.; Stern, S. T. *Methods Mol. Biol.* **2011**, *697*, 173−179.

(8) Kim, G.; Lee, Y.-E. K.; Xu, H.; Philbert, M. A.; Kopelman, R. *Anal. Chem.* **2010**, *82*, 2165−2169.

(9) Wang, X.-d.; Stolwijk, J. A.; Lang, T.; Sperber, M.; Meier, R. J.; Wegener, J.; Wolfbeis, O. S. *J. Am. Chem. Soc.* **2012**, *134*, 17011−17014.

(10) Kim, J.-H.; Heller, D. A.; Jin, H.; Barone, P. W.; Song, C.; Zhang, J.; Trudel, L. J.; Wogan, G. N.; Tannenbaum, S. R.; Strano, M. S. *Nature Chem.* **2009**, *1*, 473−481.
(11) Yuan, L.; Lin, W.; Tan, L.; Zheng, K.; Huang, W. *Angew. Chem., Int. Ed.* **2013**, *52*, 1628−1630.
(12) Chen, Y.; Zhu, C.; Yang, Z.; Chen, J.; He, Y.; Jiao, Y.; He, W.; Qiu, L.; Cen, J.; Guo, Z. *Angew. Chem., Int. Ed.* **2013**, *52*, 1688−1691.
(13) Benjaminsen, R. V.; Sun, H.; Henriksen, J. R.; Christensen, N. M.; Almdal, K.; Andresen, T. L. *ACS Nano* **2011**, *5*, 5864−5873.
(14) Peng, H.-s.; Stolwijk, J. A.; Sun, L.-N.; Wegener, J.; Wolfbeis, O. S. *Angew. Chem., Int. Ed.* **2010**, *49*, 4246−4249.
(15) Adrogué, H. J.; Madias, N. E. *N. Engl. J. Med.* **1998**, *338*, 26−34.
(16) Grinstein, S.; Swallow, C. J.; Rotsein, O. D. *Clin. Biochem.* **1991**, *24*, 241−247.
(17) Kettel, L. J.; Diener, C. F.; Morse, J. O.; Stein, H. F.; Burrows, B. *JAMA* **1971**, *217*, 1503−1508.
(18) Hood, V. L.; Tannen, R. L. *N. Engl. J. Med.* **1998**, *339*, 819−826.
(19) Tombaugh, G. C.; Sapolsky, R. M. *J. Neurochem.* **1993**, *61*, 793−803.
(20) Fang, J. S.; Gillies, R. D.; Gatenby, R. A. *Semin. Cancer Biol.* **2008**, *18*, 330−337.
(21) Harris, A. L. *Nat. Rev. Cancer* **2002**, *2*, 38−47.
(22) Bertout, J. A.; Patel, S. A.; Simon, M. C. *Nat. Rev. Cancer* **2008**, *8*, 967−975.
(23) Gulledge, C. J.; Dewhirst, M. W. *Anticancer Res.* **1996**, *16*, 741−750.
(24) Gerweck, L. E.; Seetharaman, K. *Cancer Res.* **1996**, *56*, 1194−1198.
(25) Swietach, P.; Hulikova, A.; Patiar, S.; Vaughan-Jones, R. D.; Harris, A. L. *PLoS ONE* **2012**, *7*, e35949.
(26) Gallagher, F. A.; Kettunen, M. I.; Day, S. E.; Hu, D. E.; Ardenkjaer-Larsen, J. H.; Zandt, R. I.; Jensen, P. R.; Karlsson, M.; Golman, K.; Lerche, M. H.; Brindle, K. M. *Nature* **2008**, *453*, 940−943.
(27) Kobayashi, H.; Ogawa, M.; Alford, R.; Choyke, P. L.; Urano, Y. *Chem. Rev.* **2010**, *110*, 2620−2640.
(28) Weiss, S. *Science* **1999**, *283*, 1676−1683.
(29) He, X.; Gao, J.; Gambhir, S. S.; Cheng, Z., Z. *Trends Mol. Med.* **2010**, *16*, 574−583.
(30) Weissleder, R.; Tung, C.-H.; Mahmood, U.; Bogdanov, A., Jr. *Nat. Biotechnol.* **1999**, *17*, 375−378.
(31) le Masne de Chermont, Q.; Chanéac, C.; Seguin, J.; Pellé, F.; Maîtrejean, S.; Jolivet, J.-P.; Gourier, D.; Bessodes, M.; Scherman, D. *Proc. Natl. Acad. Sci. U. S. A.* **2007**, *104*, 9266−9271.
(32) Du, J. Z.; Tang, Y. P.; Lewis, A. L.; Armes, S. P. *J. Am. Chem. Soc.* **2005**, *127*, 17982−17983.
(33) Lomas, H.; Massignani, M.; Abdullah, K. A.; Canton, I.; Lo Presti, C.; MacNeil, S.; Du, J.; Blanazs, A.; Madsen, J.; Armes, S. P.; Lewis, A. L.; Battaglia, G. *Faraday Discuss.* **2008**, *139*, 143−159.
(34) Murdoch, C.; Reeves, K. J.; Hearnden, V.; Colley, H.; Massignani, M.; Canton, I.; Madsen, J.; Blanazs, A.; Armes, S. P.; Lewis, A. L.; MacNeil, S.; Brown, N. J.; Thornhill, M. H.; Battaglia, G. *Nanomedicine* **2010**, *5*, 1025−1036.
(35) Massignani, M.; LoPresti, C.; Blanazs, A.; Madsen, J.; Armes, S. P.; Lewis, A. L.; Battaglia, G. *Small* **2009**, *5*, 2424−2432.
(36) Massignani, M.; Canton, I.; Sun, T.; Hearnden, V.; MacNeil, S.; Blanazs, A.; Armes, S. P.; Lewis, A.; Battaglia, G. *PLoS ONE* **2010**, *5*, e10459.
(37) Oliveira, H. P. M.; Camargo, A. J.; Macedo, L. G.; Gehlen, M. H.; da Silva, A. B. F. *Spectrochim. Acta A* **2002**, *58*, 3103−3111.
(38) Ngeontae, W.; Xu, C.; Ye, N.; Wygladacz, K.; Aeungmaitrepirom, W.; Tuntulani, T.; Bakker, E. *Anal. Chim. Acta* **2007**, *599*, 124−133.
(39) Grabolle, M.; Brehm, R.; Pauli, J.; Dees, F. M.; Hilger, I.; Resch-Genger, U. *Bioconjugate Chem.* **2012**, *23*, 287−292.
(40) Das, N. K.; Mandal, B. M. *Polymer* **1982**, *23*, 1653−1658.
(41) Lucarini, M.; Pedrielli, P.; Pedulli, G. F.; Valgimigli, L.; Gigmes, D.; Tordo, P. *J. Am. Chem. Soc.* **1999**, *121*, 11546−11553.
(42) Wei, Y.; Hariharan, R.; Patel, S. A. *Macromolecules* **1990**, *23*, 158−164.
(43) Jose, J.; Burgess, K. *Tetrahedron* **2006**, *62*, 11021−11037.
(44) Jose, J.; Ueno, Y.; Burgess, K. *Chem.—Eur. J.* **2009**, *15*, 418−423.
(45) Das, K.; Jain, B.; Patel, H. S. *Spectrochim. Acta A* **2004**, *60*, 2059−2064.
(46) Sabnis, R. W. *Handbook of Acid-Base Indicators*; CRC Press Inc.: Boca Raton, FL, 2007.
(47) Krihak, M.; Murtagh, M. T.; Shahriari, M. R. *J. Sol-Gel Sci. Technol.* **1997**, *10*, 153−163.
(48) Lide, D. R., Ed. *Handbook of Chemistry and Physics*, 76th ed.; CRC Press Inc.: Boca Raton, FL, 1995−1996.
(49) Bakker, E.; Lerchi, M.; Rosatzin, T.; Rusterholz, B.; Simon, W. *Anal. Chim. Acta* **1993**, *278*, 211−225.
(50) Goda, T.; Goto, Y.; Ishihara, K. *Biomaterials* **2010**, *31*, 2380−2387.
(51) Madsen, J.; Warren, N. J.; Armes, S. P.; Lewis, A. L. *Biomacromolecules* **2011**, *12*, 2225−2234.
(52) Hearnden, V.; Lomas, H.; MacNeil, S.; Thornhill, M.; Murdoch, C.; Lewis, A. L.; Madsen, J.; Blanazs, A.; Armes, S. P.; Battaglia, G. *Pharm. Res.* **2009**, *26*, 1718−1728.
(53) Acker, H. *J. Theor. Med.* **1998**, *1*, 193−207.
(54) Kunz-Schugart, L. A.; Kreutz, M.; Knuechel Int., R. *J. Exp. Pathol.* **1998**, *79*, 1−23.
(55) Mueller-Klieser, W.; Freyer, J. P.; Sutherland, R. M. *Br. J. Cancer* **1986**, *53*, 345−353.
(56) Mueller-Klieser, W. *Am. J. Physiol. Cell Physiol.* **1997**, *273*, C1109−C1123.
(57) Airley, R.; Loncaster, J.; Davidson, S.; Bromley, M.; Roberts, S.; Patterson, A.; Hunter, R.; Stratford, I.; West, C. *Clin. Cancer Res.* **2001**, *7*, 928−934.
(58) Vinci, M.; Gowan, S.; Boxall, F.; Patterson, L.; Zimmermann, M.; Court, W.; Lomas, C.; Mendiola, M.; Hardisson, D.; Eccles, S. A. *BMC Biology* **2012**, *10*, 29.
(59) Hong, S.; Leroueil, P. R.; Janus, E. K.; Peters, J. L.; Kober, M.-M.; Islam, M. T.; Orr, B. G.; Baker, J. R., Jr.; Banaszak Holl, M. M. *Bioconjugate Chem.* **2006**, *17*, 728−734.
(60) Mecke, A.; Majoros, I. J.; Patri, A. K.; Baker, J. R., Jr. *Langmuir* **2005**, *21*, 10348−10354.
(61) Canton, I.; Battaglia, G. *Chem. Soc. Rev.* **2012**, *41*, 2718−2739.
(62) Cosson, P.; de Curtis, I.; Pouysségur, J.; Griffiths, G.; Davoust, J. *J. Cell Biol.* **1989**, *108*, 377−387.
(63) Gerweck, L. E.; Seetharaman, K. *Cancer Res.* **1996**, *56*, 1194−1198.
(64) Lin, C.-W.; Shulok, J. R.; Kirley, S. D.; Cincotta, L.; Foley, J. W. *Cancer Res.* **1991**, *51*, 2710−2719.
(65) Kobayashi, H.; Choyke, P. L. *Acc. Chem. Res.* **2011**, *44*, 83−90.
(66) Wang, R.; Yu, C.; Yu, F.; Chen, L. *Trends Anal. Chem.* **2010**, *29*, 1004−1013.
(67) Escobedo, J. O.; Rusin, O.; Lim, S.; Strongin, R. M. *Curr. Opin. Chem. Biol.* **2010**, *14*, 64−70.
(68) Luo, S.; Zhang, E.; Su, Y.; Cheng, T.; Shi, C. *Biomaterials* **2011**, *32*, 7127−7138.
(69) Canton, I.; Massignani, M.; Patikarnmonthon, N.; Chierico, L.; Robertson, J.; Renshaw, S. A.; Warren, N. J.; Madsen, J. P.; Armes, S. P.; Lewis, A. L.; Battaglia, G. *FASEB J.* **2013**, *1*, 98−108.